

4.3 CIRRUS PARCEL MODEL COMPARISON PHASE 2

Ruei-Fong Lin^{1,2*}, David O’C. Starr², Paul J. DeMott³
Richard Cotton⁴, Eric Jensen⁵, Bernd Kärcher⁶ and Xiaohong Liu⁷

¹UMBC/GEST Center, Baltimore, MD, USA

²Laboratory of Atmosphere, NASA/GSFC, Greenbelt, MD, USA

³Dept. of Atmospheric Sciences, Colorado State University, Fort Collins, CO, USA

⁴Meteorological Research Flight, Hants, UK

⁵NASA/Ames Research Center, Moffett Field, CA, USA

⁶DLR Oberpfaffenhofen, Institut für Physik der Atmosphäre, Wessling, Germany

⁷Dept. of Atmospheric, Oceanic and Space Sciences, University of Michigan, MI, USA

1 Introduction

The Cirrus Parcel Model Comparison (CPMC) project, a project of the GEWEX Cloud System Study Working Group on cirrus clouds (GCSS WG2), is an international effort to advance our knowledge of numerical simulations of cirrus cloud initiation. This project was done in two phases. In Phase 1 of CPMC, the critical components determining the predicted cloud microphysical properties were identified using parcel models in which the aerosol and ice crystal size distributions are explicitly resolved (Lin et al., 2002); e.g., the formulation of the homogeneous freezing of aqueous solution droplets, especially the gradient of nucleation rate with respect to solution concentration; aerosol growth modeling; and the mass accommodation coefficient of water vapor on ice surface (the deposition coefficient). In Phase 1, all simulations were conducted using a given background aerosol distribution. To complete the comparison study, participant model responses to a range of background aerosol distributions are investigated in Phase 2.

2 Protocol

As in Phase 1, the background aerosol distributions are here assumed to be log-normal. Five sets of simulations are conducted to test the sensitivity of predicted cirrus microphysical properties to the assumed aerosol distributions and freezing property by varying the aerosol total number concentration N_t ,

mode radius r_g , distribution width σ , and λ . The empirical parameter λ (Sassen and Dodd, 1988) accounts for the non-ideal ionic effect on the freezing temperature and is adopted in quite a few models to calculate homogeneous nucleation rates (Table 1).

Table 1: Background aerosol size distributions $N(r)dr = \frac{N_t}{\sqrt{(2\pi)\ln\sigma}} \exp[-\frac{1}{2}(\frac{\ln r - \ln r_g}{\ln\sigma})^2]d\ln r$ and the value of λ .

identifier	N_t [cm ⁻³]	r_g [μm]	σ	λ
CTRL	200	0.2	1.8	2
FVFD	1000	0.2	1.8	2
MRSB	200	0.4	1.8	2
SGMA	200	0.2	2.3	2
LMBD	200	0.2	2.3	1

Parcels were assumed to be ice saturated initially and are lifted by updrafts of 3 different strengths (0.04, 0.2, 1 m s⁻¹) from initial temperatures of -40°C (340 mb; the warm cases) and -60°C (170 mb; the cold cases). Participants were asked to set the deposition and condensation coefficients to 0.5 (Haynes et al, 1992) and 0.06 (Shaw and Lamb, 1999), respectively.¹ Since these two coefficients are fixed, it is expected that the differences in aerosol modeling among the models will be the dominant factor controlling inter-model differences. Six models [C (R. Cotton), D (P. J. DeMott), J (E. Jensen), K (B. Kärcher), L (R.-F. Lin), and X (X. Liu)] participated in Phase 2. A detailed description of these

*Corresponding author’s address: Ruei-Fong Lin, UMBC/GEST Center, NASA/GSFC, Code 912, Greenbelt, MD, 20771; E-Mail: lin@agnes.gsfc.nasa.gov

¹Model J set the deposition coefficient equal to 1. From sensitivity tests done in Phase 1, the impact on the predicted N_i by varying the deposition coefficient from 0.5 to 1 is small.

models can be found in Lin et al. (2002).

3 Preliminary results

Inter-model differences were reduced compared to Phase 1 because all models adopted the same value of deposition coefficient in Phase 2. The 0.2 m s^{-1} updraft runs in the SGMA simulation set is the same as the λ -fixed run in the Phase 1 except for the deposition coefficient requirement. The maximum inter-model differences in the predicted ice particle number concentration N_i for the former (SGMA) is about a factor of 5 whereas the latter (λ -fixed) is about a factor of 25. However, the inter-model differences were still significant in some cases. In most cases, especially for the cold cases, models C, K, and X obtained larger ice particle number concentration N_i than models D, J, and L. Because of the bifurcation in the predicted N_i , models are grouped accordingly, and the average of each group is shown in Figure 1.

The logarithm of the predicted N_i quasi-linearly increases with the logarithm of updraft speed in every case. Values of N_i span more than two orders of magnitude for a given range of updraft speed. For a given updraft, N_i is greater in the cold cases.

The two groups predicted similar N_i for the warm cases when the updraft is weak. However, the difference increases slightly with updraft speed. Similarly, in the cold cases, the difference is smallest when updraft is weak and increases with updraft speed. Note, however, that the difference is much greater in the cold cases.

In Figure 2, the predicted N_i of the FVFD, MRSH, and SGMA runs are compared with the corresponding CTRL runs, while the predicted N_i of LMBD runs are compared with the corresponding SGMA runs. The differences exceed 100% only in the cold cases for FVFD with 1 m s^{-1} updraft scenario simulated by model C and MRSH with 0.2 to 1 m s^{-1} updraft scenarios simulated by models C and X. The differences in N_i between two runs for a given model (Fig.2) are small compared to model-to-model variability (Fig.1). This seems to indicate that aerosol distribution may be of secondary importance, at least for the range of aerosol distributions studied in this project.

In general, the response to the variation in the aerosol distribution in the warm cases is smaller than the cold cases. An increase in the aerosol number concentration or mode radius results in an increase in the N_i , except for model D in the warm and weak updraft scenario.

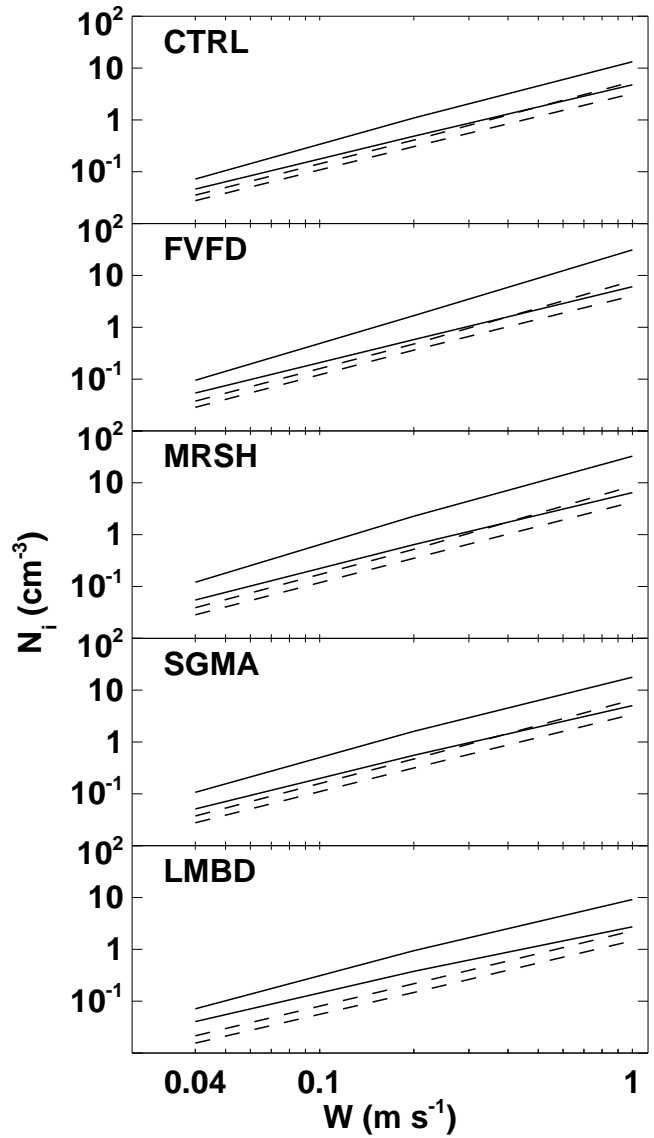


Figure 1: The predicted N_i vs. updraft speed. The cold cases are indicated by the solid-line couplets, while the warm cases are denoted by the dashed-line couplets. For a given line couplet, the upper curve is the average of models C, K, and X; the lower is the average of models D, J, and L.

Models respond to the increase in aerosol distribution width differently. Models D and J predicted smaller N_i in SGMA while the other models obtained larger N_i . For the LMBD runs, a smaller N_i was predicted by models C, L, and X. In contrast, in the cold cases, model D produced more N_i in LMBD runs. Roughly speaking, a stronger updraft induced a stronger model response to aerosol distribution and

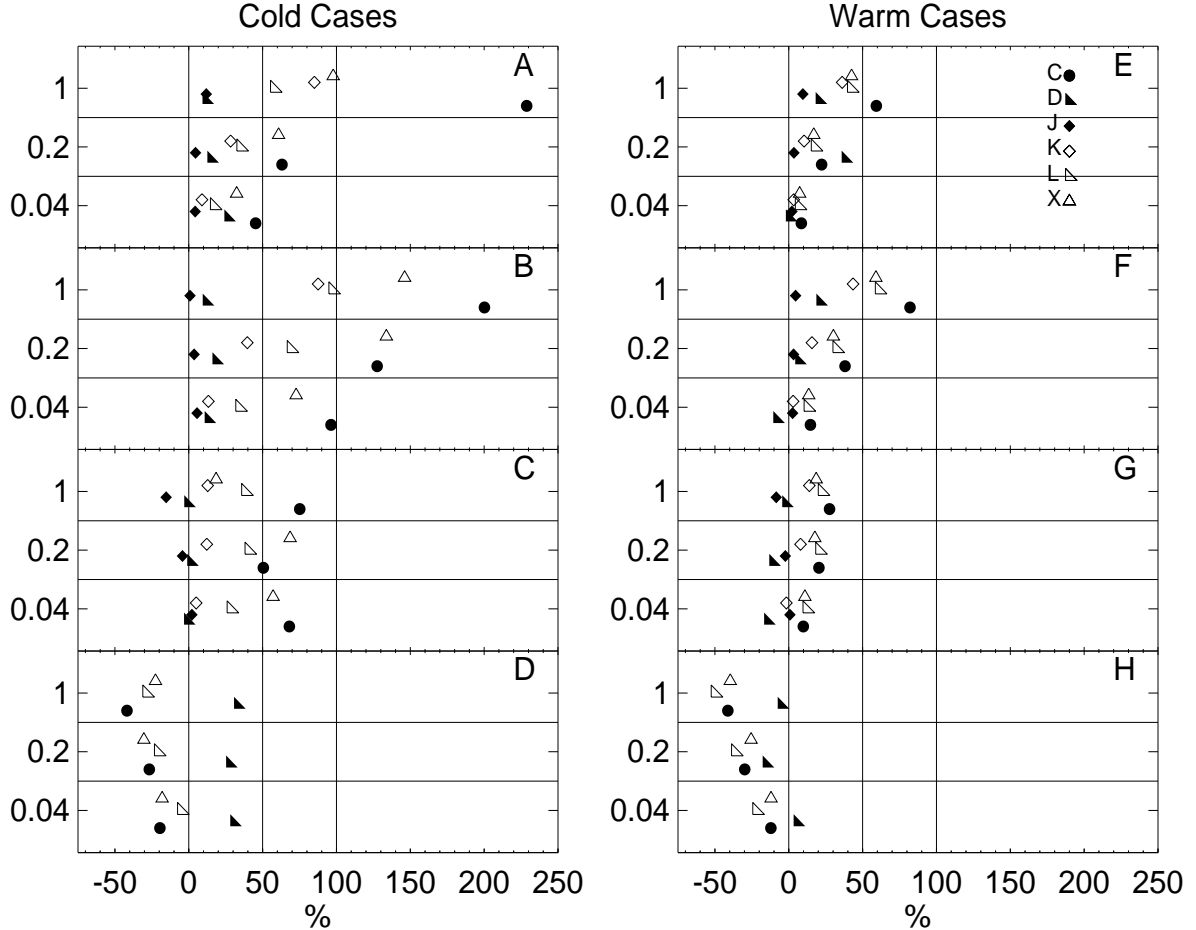


Figure 2: The differences in N_i between two runs. The labels 0.04, 0.2, 1.0 are the imposed updraft speeds. Panels A and E: $[N_i(\text{FVFD})/N_i(\text{CTRL}) - 1] \times 100\%$. Panels B and F: $[N_i(\text{MRSH})/N_i(\text{CTRL}) - 1] \times 100\%$. Panels C and G: $[N_i(\text{SGMA})/N_i(\text{CTRL}) - 1] \times 100\%$. Panels D and H: $[N_i(\text{LMBD})/N_i(\text{SGMA}) - 1] \times 100\%$. Models J and K did not submit LMBD runs.

properties. However, there are exceptions. For example, the effect of aerosol distribution is not sensitive to W in model J and only weakly sensitive in model D. Similarly, the effects of σ are weakly dependent on W in the warm cases and mixed in the cold cases.

4 Discussion

The grouping of models according to N_i may have resulted from a combination of reasons. It has been shown in Phase 1 that when models explicitly compute the diffusional growth of haze particles, large haze particles (the ones that contain more solute mass) can deviate significantly from their equilibrium sizes at low temperatures and strong uplift. The most dilute particles are not necessarily the

largest ones. Therefore, at the beginning of the nucleation regime, homogeneous freezing takes place at the mid-size haze particles and the ice particle formation rates (dN_i/dt) are much greater than if assuming equilibrium-sized haze particle growth. Quite interestingly, models C, K, L and X explicitly compute the diffusional growth of haze particles; yet model L is grouped with models D and J in terms of predicted N_i . A numerical factor may offer the explanation. The smallest bin of ice crystals is set to about 1 ($1.6 \mu\text{m}$ in model L (D)); while the resolved ice crystal distributions in other models cover the size of newly frozen haze droplets. The gap between the smallest size bin and the actual freezing size of haze particles increases with decreasing temperature because haze particles freeze at lower humidity and thus, smaller sizes. Furthermore, for a given deposition coefficient, sub-micron-sized ice crystals grow

slower at lower temperatures. As a result, this numerical factor has stronger impact on N_i at colder temperatures.

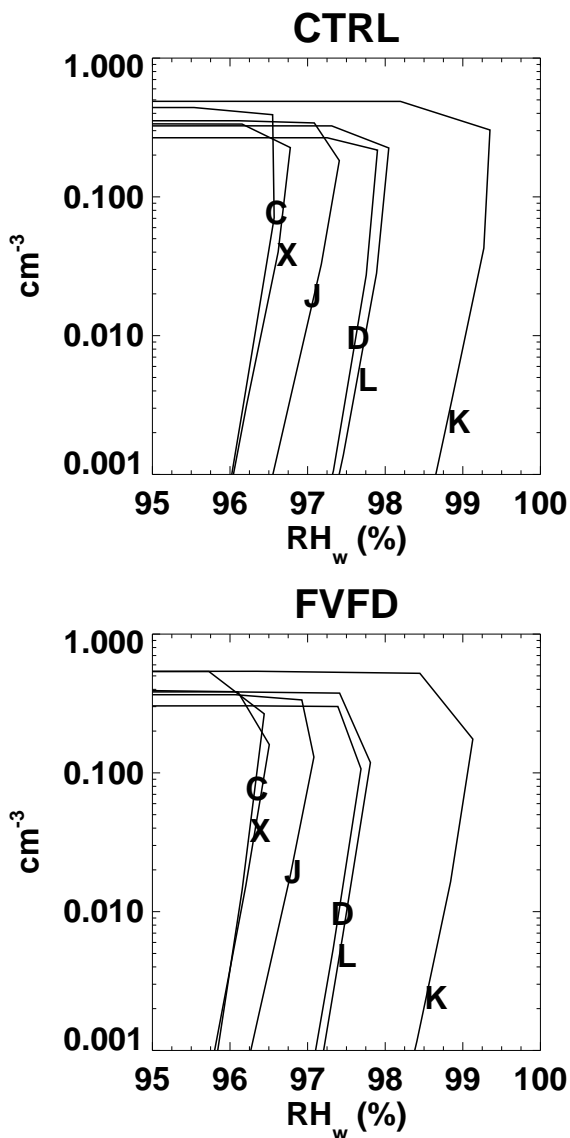


Figure 3: The evolution of N_i with respect to RH_w when the updraft is 0.2 m s^{-1} and the starting temperature is -40°C .

The mechanisms by which the changes in aerosol distribution affect the predicted cloud microphysics are complicated. Here, only the comparison of FVFD and CTRL runs are discussed. For the cases that homogeneous nucleation of haze particles is the dominant nucleation mode and the vertical displacement of the ascending parcel is large enough, Heymsfield and Sabin (1989) and Jensen et al. (1994) reported a weak response of the predicted N_i to the

change of aerosol number concentration. This weak response contrasts the stronger Twomey effect in the stratocumulus clouds. However, the reasons for the weak response in cirrus regime are not fully understood.

Roughly speaking, N_i exponentially increases with relative humidity with respect to water RH_w before the parcel reaches its peak RH_w . We may arbitrarily define a threshold RH_w , above which the homogeneous freezing of haze particles become effective (Fig 3). From the equation governing the ice particle formation rate and assuming that haze particles are in equilibrium with the environment, the change of aerosol number concentration alone does not affect the slope ($d \ln N_i / d RH_w$) of these curves. The change in N_t only alters the threshold RH_w . This might be one of the reasons responsible for the weak response. In such a case with smaller N_t and a higher threshold RH_w , ice crystals may grow faster once nucleated because of higher RH_i . As a result of enhanced moisture uptake, nucleation shuts off more quickly when N_i is smaller.

5 ACKNOWLEDGMENT

The U.S. DOE ARM Program and NASA Radiation Sciences Program have provided direct support (RFL and DS) for this GCSS project. We thank support from UK Met. Office (RC), NSF-ATM0071321 (PJD), NASA's Stratospheric Aerosol and Gas Experiment (EJ), the HGF-BMBF project Particles and Cirrus Clouds (BK), and the NASA ACMAP program (XL).

6 Reference

- Haynes, D. R., N. J. Tro, and S. M. George, Condensation and evaporation of H_2O on ice surfaces. *J. Phys. Chem.*, **96**, 8502-8509, 1992.
- Heymsfield, A. J., and R. M. Sabin, Cirrus crystal nucleation by homogeneous freezing of solution droplets. *J. Atmos. Sci.*, **46**, 2252-2264, 1989.
- Jensen et al., Microphysical modeling of cirrus 2. Sensitivity studies. *J. Geophys. Res.*, **99**, 10,443-10,454, 1994.
- Lin, R.-F., D. O'C. Starr, P. J. DeMott, R. Cotton, K. Sassen, E. Jensen, B. Kärcher, and X. Liu, Cirrus parcel model comparison phase 1. The Critical components to simulate cirrus initiation explicitly. *J. Atmos. Sci.*, accepted, 2002.
- Sassen, K., and G. C. Dodd, Homogeneous nucleation rate for highly supercooled cirrus cloud droplets. *J. Atmos. Sci.*, **45**, 1357-1369, 1988.
- Shaw, R. A., and D. Lamb, Experimental determination of the thermal accommodation and condensation coefficients of water. *J. Chem. Phys.*, **111**, 10659-10663, 1999.